RESEARCH ARTICLE Indian Journal of Agricultural Research, Volume 59 Issue 10: 1608-1618 (October 2025)

# Green Synthesis of Nanoparticles using Pea Peel Biomass and Their Assessment on Seed Germination of Tomato, Chilli and Brinjal Crop

Anjali Kanwal[1], Bikram Jit Singh[2], Suresh Kumar[3], Rippin Sehgal[4], Sushil Kumar Upadhyay[1], Raj Singh[1]

10.18805/IJARe.A-6301

## ABSTRACT

**Background:** Modern agriculture heavily relies on chemical fertilizers, which can harm the ecosystem. Applying fertilizers based on nanoparticles (NPs) topically at ppm levels provides a faster and more efficient way to capture essential nutrients for plant growth and development. The "green" synthesis of NPs has become more and more popular as a means of achieving sustainability and environmental protection. Nano-fertilizers have been used to increase crop yields.

**Methods:** In the present study, zinc, iron and manganese NPs were green synthesized and characterized. Their aqueous solution assessment was also carried out on the tomato, chilli and brinjal crop seed germination. The extract of the pea peel biomass is used as the reducing agent to synthesize ZnO, $Fe_2O_3$ and $MnO_2$ NPs. The triplicates of each crop, consisting of sterilized 20 tomato, chilli and brinjal seeds, were sprayed with ZnO, $Fe_2O_3$ and $MnO_2$ NPs at varying concentrations (10, 20 and 50 *ppm*).

**Result:** Through peak-matching and the formation of an FT-IR band in the 400-800 $cm^{-1}$ region, XRD examination verified that the NPs were produced. UV-visible spectroscopy proved the particles' direct band gap nature, whereas FE-SEM showed their spherical shape, agglomerated multiform and globular dispersion. The particles' diameters ranged from 40 to 120 nm. The maximum germination frequency (25.00) of brinjal seeds was observed in Mn with seed vigour (88.33), followed by ZnFeMn (23.75) and Zn (22.50) NPs for 20 *ppm*. Zn was found effective for germination in all crop seeds with germination frequency (20.00 to 22.50). This study demonstrated the importance of green nanoparticles, which are economical and environmentally benign, on seed germination. Therefore, we must develop new approaches to address various challenges and ensure sufficient food for everyone. A useful tool for assisting farmers in implementing new techniques and guaranteeing steady agricultural yields is nanotechnology.

**Key words:** Fe-SEM, Ft-Ir, Nanoparticles, Seeds germination, Uv-visible spectroscopy, Vigour.

## INTRODUCTION

The productivity and nutrient efficiency of agricultural fields can be greatly enhanced by nanotechnology. The enhanced nutrient absorption capacity of plant roots by the nano-fertilizers promotes photosynthesis and raises agricultural output (INIC, 2014). However, applying nutrients based on nanoparticles (NPs) topically provides a faster and more efficient way to absorb essential nutrients. "Green" NPs synthesis has becoming more and more popular as a means of achieving sustainability and environmental protection. Nano-fertilizers with *ppm* levels of manganese oxide ($MnO_2$), iron oxide ($Fe_2O_3$) and zinc oxide (ZnO) nanoparticles have been used to increase crop yields (Wang *et al.,* 2004).

ZnO has been approved as safe and non-toxic by the US Food and Drug Administration (Bala *et al.,* 2015; Khaleghi *et al.,* 2022). For the synthesis of ZnO nanoparticles, biological approaches seem to be more adaptable than physical and chemical procedures due to their simplicity, biocompatibility and environmental friendliness (Kajbafvala *et al.,* 2012). Zinc is considered an essential element in plants because it plays a significant role in many aspects of seed germination and growth (Sheoran *et al.,* 2024). But an excess of zinc can cause physiological, metabolic and morphological issues (Balafrej *et al.,* 2020).

[1]Department of Bio-Sciences and Technology, Maharishi Markandeshwar (Deemed to be University), Mullana, Ambala-133 207, Haryana, India.
[2]Department of Mechanical Engineering, Maharishi Markandeshwar (Deemed to be University), Mullana, Ambala-133 207, Haryana, India.
[3]Department of Physics, Maharishi Markandeshwar (Deemed to be University), Mullana, Ambala-133 207, Haryana, India.
[4]Department of Biotechnology, Ambala College of Engineering and Applied Research, Devsthali, Ambala-133 001, Haryana, India.

**Corresponding Author:** Raj Singh, Department of Bio-Sciences and Technology, Maharishi Markandeshwar (Deemed to be University), Mullana, Ambala-133 207, Haryana, India.
Email: dr.rajsingh09@gmail.com

**How to cite this article:** Kanwal, A., Singh, B.J., Kumar, S., Sehgal, R., Upadhyay, S.K. and Singh, R. (2025). Green Synthesis of Nanoparticles using Pea Peel Biomass and Their Assessment on Seed Germination of Tomato, Chilli and Brinjal Crop. *Indian Journal of Agricultural Research*. **59(10):** 1608-1618. doi: 10.18805/IJARe.A-6301.

**Submitted:** 21-08-2024 **Accepted:** 15-01-2025 **Online:** 18-02-2025

Iron (Fe) is the only trace metal required for plant growth and development. According to Lin *et al*. (2019), it is necessary for physiological and biochemical functions such as respiration, photosynthesis and cell metabolism.

Despite being abundant in soil, iron is difficult for plants to absorb due to its insolubility. Chlorosis and reduced biomass are common symptoms of iron deficiency in plants (Hindt and Guerinat, 2012). Finding inexpensive and sustainable methods to apply NPs as fertilizer to plants suffering from iron deficiency-induced chlorosis is vital (Cieschi *et al.,* 2019).

Manganese oxide nanoparticles (NPs) are of interest to researchers due to their unique chemical, biological, physical and photocatalytic properties (Gevers *et al.,* 2022). Additionally, $MnO_2$ NPs can be used to make bactericides and as components of fertilizers (Ogunyemi *et al.,* 2019). Nanomaterials, especially manganese nanoparticles and their oxides, are used extensively in agriculture (Hassanisaadi *et al.,* 2022).

The Solanaceae family includes eggplant (*Solanum melongena* L.), tomatoes (*Solanum lycopersicum* L.) and chilies (*Capsicum annuum*). Grown all over the world for their nutritional and medicinal qualities. Tomatoes are rich in potassium, carbohydrates and ascorbic acid, as well as antioxidants such tocopherols and lycopene. Tomato fruit has several health benefits, including a decreased risk of heart disease (Renna *et al.,* 2018). The mineral and nutritional composition of eggplant fruits, which contains vitamins A and B, is well-known. They are also heavy in iron and low in protein and carbohydrates.

Plant extract has been found to be the most effective stabilizing and reducing agent for the green synthesis of nanoparticles. Green nanofertilizers have the potential to improve soil fertility, agricultural productivity and reduce environmental pollution caused by traditional fertilizers.

Green nanofertilizers increase their effectiveness by focusing on specific areas of plant tissues. By capturing light, the NPs accelerate photosynthesis and produce dry matter, which enhances plant growth and output. Enhancing crop yield and promoting sustainable farming can be accomplished with these eco-friendly nano-fertilizers.

In this work, we employed biomass extract from pea peels to produce green nanoparticles that were biologically produced, evaluated for zinc, iron and manganese oxide NPs and investigated for the germination of tomato, chilli and brinjal seeds. These nanoparticles can be helpful in this field since they are smaller and have a higher surface area than the corresponding bulk metals and metal oxides.

## MATERIALS AND METHODS

The research was carried out in the Department of the Bio-sciences and Technology in Maharishi Markandeshwar (Deemed to be University) Mullana, Ambala, Haryana, India; in February 2023 (30.2753 °N, 77.0476 °E). The seeds (brinjal, tomato and chilli) were purchased from a neighborhood market in Barara, Ambala. After sufficiently sterilizing their surfaces, the seeds were cleaned with distilled water to get rid of any small dust particles before being utilized in additional experiments.

### Pea peel collection and extract

The plant biomass used is pea (*Pisum sativum* L.) peel. The 25 g of pea peel was added to a 100 ml beaker that had 50 ml of double-distilled water. The aforementioned combination was then heated to 60°C for ten minutes while being constantly swirled with a hot stirrer plate. After the stirring period was over, the mixture was allowed to cool to ambient temperature before being filtered using Whatman No. 1 filter paper and kept for later use at 4°C (Narayanamma *et al.,* 2016).

### Synthesis of ZnO, $Fe_2O_3$ and $MnO_2$ NPs

Precursors zinc acetate (Zn $(CH_3COO_2.2H_2O)$, Ferric chloride $(FeCl_3.6H_2O)$ and Manganese acetate Mn $(CH_3COO)$ $2.6H_2O$) were utilized for the synthesis of ZnO, $Fe_2O_3$ and $MnO_2$ NPs respectively. Three 250 ml beakers containing 9, 40 and 180 ml of pea peel extract were mixed with 0.219, 0.270 and 0.122 g of Zn, Fe and Mn precursors respectively using hot plate magnetic stirring at 70°C and the solution was agitated. Next, a 2 M sodium hydroxide (NaOH) solution was gradually added until the *p*H values of the solutions reached to 12, 11 and 8 respectively. After allowing the solution to settle to ambient temperature, repeatedly distilled water was added to wash the NPs and the 7 *p*H was obtained. The solutions were firstly centrifuged at 10000 *rpm* for 10 min. Then precipitate of NPs filtered *via* Whatman filter number 1 and dried overnight at 40°C (for Zn sample) and 80°C (Fe and Mn samples) (Ustun *et al.,* 2022).

### Characterization of ZnO, $Fe_2O_3$ and $MnO_2$ NPs

The synthesized NPs were tracked using a UV-visible spectrophotometer (Shimadzu 2600) for optical properties. FT-IR spectra were collected at 400-4000 $cm^{-1}$ wavelengths using an FTIR spectrophotometer (Shimadzu 8400) to examine the presence of functional groups. To get ready the pellet for FT-IR analysis about 2 mg of the NPs were combined with KBr. Using an XRD diffractometer (XRD-Bruker), the crystalline size and purity of NPs were determined. Field emission scanning electron microscopy (FE-SEM: Zeiss Sigma 3) was used to examine the surface features of the biosynthesized NPs.

### Seed germination

To assess germination 20-20 tomato, chilli and brinjal seeds were placed in the plates that had been lined with blotting paper. Plates were covered and placed in a seed germinator (SSI) for 7 days (Siddiqui and Al-Whaibi, 2014). Each plate had 5 ml of water supplied on the second, fourth and sixth days of germination. The seeds were sprayed three times (every 48 hours) with stickers and varying quantities of nanoparticles. 10, 20 and 50 *ppm* concentrations of nanoparticle suspensions singly as well as in combinations (doubled and triples) were added in each plate of seeds. The mean germination frequency, seed vigour and germination percentage were further calculated (Arora *et al.,* 2024).

### Statistical analysis

The continuous variables, represented as mean ± standard deviation (SD), were applied to categorical variables. To determine statistically significant changes between the tested extract and the standard, analysis of variance (ANOVA) was utilized. Version 21 of the SPSS software was used to conduct the statistical analysis. Critical differences were computed at the $p$ = 0.05 level after single-way ANOVA)was performed on data from three replications.

## RESULTS AND DISCUSSION

### Green synthesis

The production of ZnO NPs was suggested by the reaction mixture's color changing from pale yellow to pale white precipitate, which verified the presence of zinc (Thi *et al.,* 2021). The reaction mixtures changed from brown to dark brown, confirming the presence of iron (Ustun *et al.,* 2022). The reaction mixture changed from pale white to brown, indicating the presence of manganese (Hoseinpour *et al.,* 2018).

### UV-visible spectroscopy

In the present study, the UV-visible absorption spectra of the biosynthesized ZnO, $Fe_2O_3$ and $MnO_2$ NPs are recorded for wavelength 200-700 nm (Fig 1a). All the biosynthesized NPs revealed a broad absorption band between 250-380 nm in the UV-region that indicated their strong ability to absorb UV light. Although, $Fe_2O_3$ and $MnO_2$ NPs both have excellent visible light absorption features between 400-700 nm than ZnO NPs (Fig 1a). The optical band gap energies (*E*g, eV) of the biosynthesized NPs have been estimated by extrapolating the straight line to the horizontal axis in the high absorption region (Fig 1b) using the Tauc plot method for direct (Kumar *et al.,* 2020). The calculated *E*g values for the ZnO, $Fe_2O_3$ and $MnO_2$ NPs are found to be 3.17 eV, 2.11 eV and 2.01 eV respectively. These values are also consistent with the published literature (Kumar *et al.,* 2020).

### Field emission scanning electron microscopy (FE-SEM)

FE-SEM micrographs of biosynthesized ZnO, $Fe_2O_3$ and $MnO_2$ NPs (Fig 2a-c) displayed irregular-sized, agglomerated and globular ranged assemblies. FE-SEM images are further analyzed for the particle size frequency count using ImageJ software as shown in Fig 2d-f. FE-SEM images (Fig 2a-c) displayed that the largest grain size is observed in $MnO_2$ NPs (20-300 nm having an average size of ~115 nm) while it has uniform smallest nano assemblies of the particles. However, for $Fe_2O_3$ NPs larger grains in irregular size (20-160 nm with an average of ~75 nm) are formed. In the case of ZnO NPs, irregular assemblies along with a few hexagonal shapes (20-160 nm with an average of 47 nm) are observed.

### X-ray diffraction (XRD)

In the XRD pattern (Fig 3 a-c), the diffraction peaks that appeared at different 2$\theta$ positions indexed for corresponding (*hkl*) values for ZnO, $Fe_2O_4$ and $MnO_2$ nanoparticles are matched well with JCPDS card 031-1451, 89-596 and 44-0141 respectively (Kumar *et al.,* 2020). Also, a hexagonal type wurtzite structure for polycrystalline ZnO nanoparticles oriented along (101) reflection plane, a hematite structure for $\alpha$-$Fe_2O_3$ having a prominent (104) reflection plane and a tetragonal structure for $\alpha$-$MnO_2$ with crystallites orientation in (100) plane has been observed. Furthermore, the average size of crystallites was calculated from Debye-Scherer's equation (Kumar *et al.,* 2020) and was found to be 40.14 nm for ZnO, 23.21 nm for $Fe_2O_3$ and 18.84 nm for $MnO_2$ nanoparticles.

### Fourier-transform infrared (FT-IR) spectroscopy

FT-IR spectra for biosynthesized ZnO, $Fe_2O_3$ and $MnO_2$ NPs were displayed in Fig 3d-f. All the samples have a strong and broad absorption band between wavenumber ~3400-3430 $cm^{-1}$ that results from the hydrogen bonding of O-H groups between $H_2O$ molecules. It is also an indication for the presence of water or moisture content on the surface of nanoparticles and is further supported by the detection

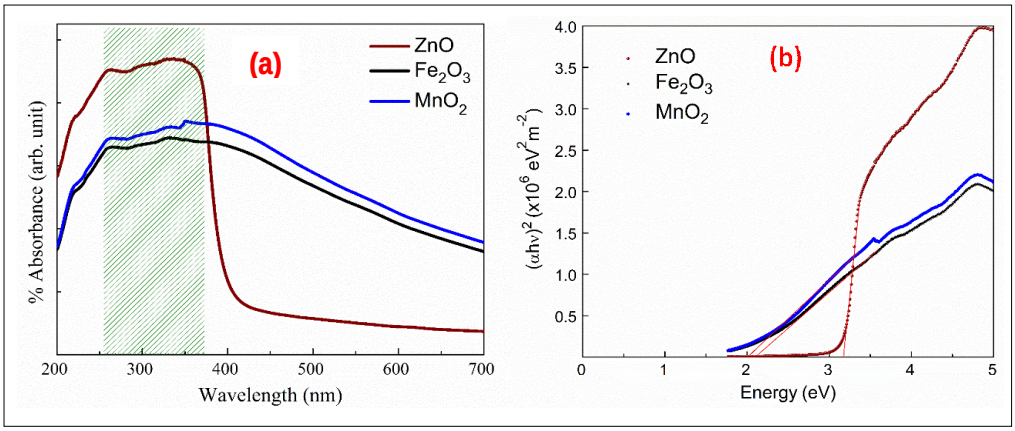



**Fig 1:** (a) UV-visible absorption spectra and (b) Tauc plot for direct band gap of the biosynthesized ZnO, $Fe_3O_4$ and $MnO_2$ NPs using pea peel extract.

of O-H bending vibration at ~1600-1630 $cm^{-1}$ and ~1030-1060 $cm^{-1}$. In case of ZnO and $Fe_2O_3$ (Fig 3d, e), the-$CH_3$ vibration at ~1380 $cm^{-1}$ ascribed to the alkane group of phytochemicals also observed. For $MnO_2$ NPs, (Fig 3f), strong absorption bands at 860, 1415 and 1589 $cm^{-1}$ are observed which are ascribed to C-H out of plane, C-O stretch of carboxylic acid and asymmetric/symmetric C=O stretching (Shatnawi *et al.,* 2016). A strong absorption band observed at 480 $cm^{-1}$ is ascribed for Zn-O stretching vibrations (Fig 3d), double bands at 461 $cm^{-1}$ and 618 $cm^{-1}$ are attributed to Fe-O-Fe stretching (Fig 3e) and a band at 613 $cm^{-1}$ primarily assigned to Mn-O-Mn vibration modes in $MnO_2$ (Fig 3f). Moreover, the characteristics absorption bands correspond to ZnO, $Fe_2O_3$ and $MnO_2$ NPs are well matched with the reported literature (Keshri and Biswas, 2022).

**Effect of nanoparticles on seed germination**

The maximum germination frequency (25.00) of brinjal seeds was observed in MnO NPs with seed vigour (88.33), followed by ZnFeMn (23.75) and Zn (22.50) NPs for 20 ppm and also in case of 10 ppm ZnO (21.25). The 50 ppm concentration was found less effective on seed

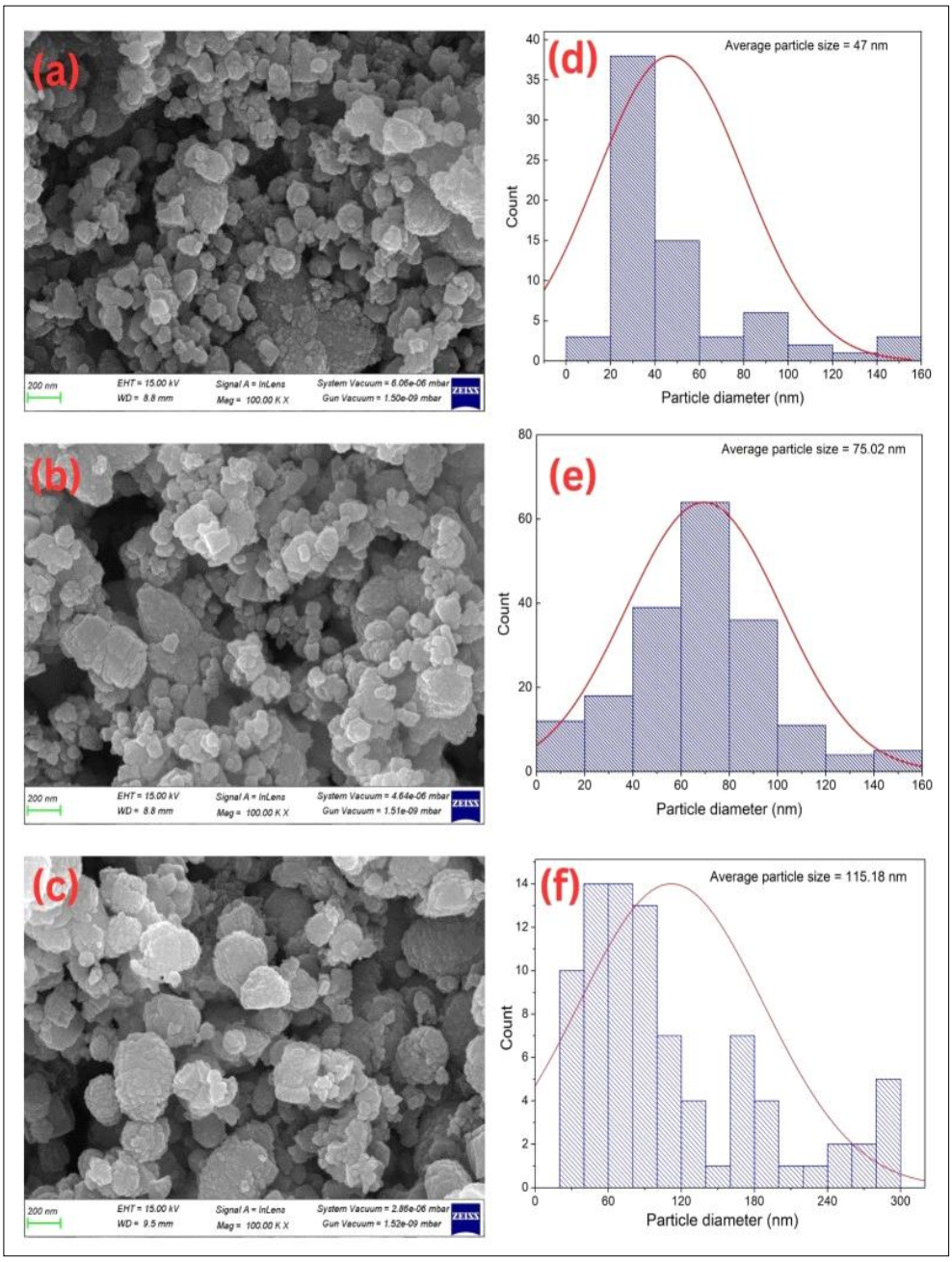



**Fig 2:** FE-SEM pattern (a-c) and corresponding particle size distribution curves (d-f) for the ZnO, $Fe_3O_4$ and $MnO_2$ NPs that are biosynthesized using pea peel extract.

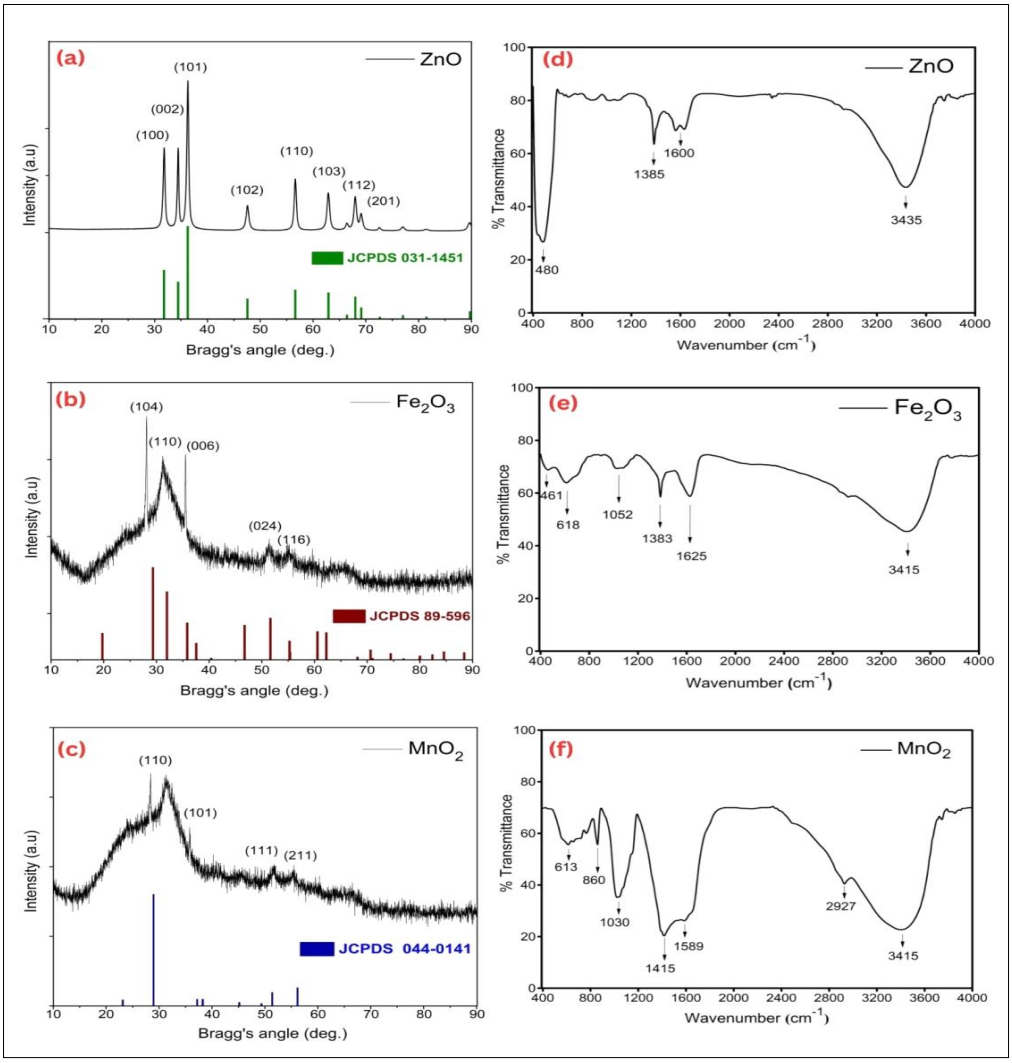



**Fig 3:** XRD pattern (a-c) and FT-IR spectra (d-f) for ZnO NPs, $Fe_3O_4$ and $MnO_2$ NPs that are biosynthesized using pea peel extract.

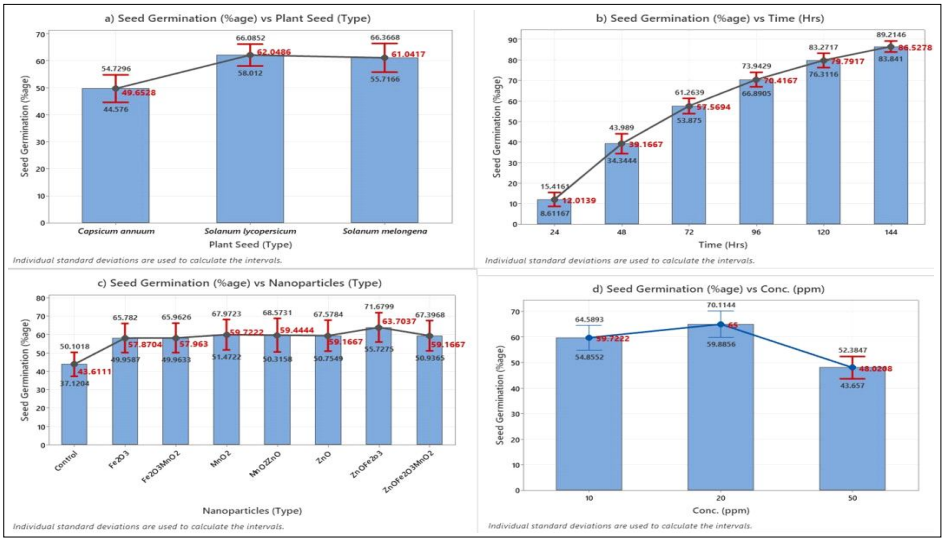



**Fig 4:** Error-bar plots for considered variables.

germination. Therefore, the maximum seed germination frequency was observed with 20 *ppm* concentration of all single, double and triple combinations followed by 10 *ppm*.

The maximum germination frequency (20.00) of tomato seeds was observed in ZnFe, Zn and MnZn (19.00) NPs for 20 *ppm* and followed by ZnFeMn and Zn (18.00) for 10 *ppm*.

**Table 1:** Regression equations for seed germination % age.

| Plant seed (Type) | Nanoparticles (Type) | | | |
|---|---|---|---|---|
| *Capsicum annuum* | Control | Seed germination (%age) | = | -5.56+ 0.6039 Time (Hrs)- 0.3556 Conc. (*ppm*) |
| *Capsicum annuum* | $Fe_2O_3$ | Seed germination (%age) | = | 8.70 + 0.6039 Time (Hrs)- 0.3556 Conc. (*ppm*) |
| *Capsicum annuum* | $Fe_2O_3$ $MnO_2$ | Seed germination (%age) | = | 8.79 + 0.6039 Time (Hrs)- 0.3556 Conc. (*ppm*) |
| *Capsicum annuum* | $MnO_2$ | Seed germination (%age) | = | 10.55 + 0.6039 Time (Hrs)- 0.3556 Conc. (*ppm*) |
| *Capsicum annuum* | $MnO_2$ ZnO | Seed germination (%age) | = | 10.27 + 0.6039 Time (Hrs)- 0.3556 Conc. (*ppm*) |
| *Capsicum annuum* | ZnO | Seed germination (%age) | = | 9.99 + 0.6039 Time (Hrs)- 0.3556 Conc. (*ppm*) |
| *Capsicum annuum* | ZnO $Fe_2O_3$ | Seed germination (%age) | = | 14.53 + 0.6039 Time (Hrs)- 0.3556 Conc. (*ppm*) |
| *Capsicum annuum* | ZnO $Fe_2O_3$ $MnO_2$ | Seed germination (%age) | = | 9.99 + 0.6039 Time (Hrs)- 0.3556 Conc. (*ppm*) |
| *Solanum lycopersicum* | Control | Seed germination (%age) | = | 6.83 + 0.6039 Time (Hrs)- 0.3556 Conc. (*ppm*) |
| *Solanum lycopersicum* | $Fe_2O_3$ | Seed germination (%age) | = | 21.09 + 0.6039 Time (Hrs)- 0.3556 Conc. (*ppm*) |
| *Solanum lycopersicum* | $Fe_2O_3$ $MnO_2$ | Seed germination (%age) | = | 21.19 + 0.6039 Time (Hrs)- 0.3556 Conc. (*ppm*) |
| *Solanum lycopersicum* | $MnO_2$ | Seed germination (%age) | = | 22.94 + 0.6039 Time (Hrs)- 0.3556 Conc. (*ppm*) |
| *Solanum lycopersicum* | $MnO_2$ ZnO | Seed germination (%age) | = | 22.67 + 0.6039 Time (Hrs)- 0.3556 Conc. (*ppm*) |
| *Solanum lycopersicum* | ZnO | Seed germination (%age) | = | 22.39 + 0.6039 Time (Hrs)- 0.3556 Conc. (*ppm*) |
| *Solanum lycopersicum* | ZnO $Fe_2O_3$ | Seed germination (%age) | = | 26.93 + 0.6039 Time (Hrs)- 0.3556 Conc. (*ppm*) |
| *Solanum lycopersicum* | ZnO $Fe_2O_3$ $MnO_2$ | Seed germination (%age) | = | 22.39 + 0.6039 Time (Hrs)- 0.3556 Conc. (*ppm*) |
| *Solanum melongena* | Control | Seed germination (%age) | = | 5.83 + 0.6039 Time (Hrs)- 0.3556 Conc. (*ppm*) |
| *Solanum melongena* | $Fe_2O_3$ | Seed germination (%age) | = | 20.09 + 0.6039 Time (Hrs)- 0.3556 Conc. (*ppm*) |
| *Solanum melongena* | $Fe_2O_3$ $MnO_2$ | Seed germination (%age) | = | 20.18 + 0.6039 Time (Hrs)- 0.3556 Conc. (*ppm*) |
| *Solanum melongena* | $MnO_2$ | Seed germination (%age) | = | 21.94 + 0.6039 Time (Hrs)- 0.3556 Conc. (*ppm*) |
| *Solanum melongena* | $MnO_2$ ZnO | Seed germination (%age) | = | 21.66 + 0.6039 Time (Hrs)- 0.3556 Conc. (*ppm*) |
| *Solanum melongena* | ZnO | Seed germination (%age) | = | 21.38 + 0.6039 Time (Hrs)- 0.3556 Conc. (*ppm*) |
| *Solanum melongena* | ZnO $Fe_2O_3$ | Seed germination (%age) | = | 25.92 + 0.6039 Time (Hrs)- 0.3556 Conc. (*ppm*) |
| *Solanum melongena* | ZnO $Fe_2O_3$ $MnO_2$ | Seed Germination (%age) | = | 21.38 + 0.6039 Time (Hrs)- 0.3556 Conc. (*ppm*) |

The 50 *ppm* concentration was found less effective on seed germination. Therefore, the maximum seed germination frequency was observed with 20 *ppm* concentration of all single, double and triple combinations followed by 10 *ppm* in some cases. The maximum seed vigour was observed with 20 and 10 *ppm* concentrations in ZnFe (76.66), Zn (71.66) and ZnFeMn (71.66) respectively, as compared to other treatments. The maximum germination frequency (22.50) of chilli seeds was observed in Zn and MnZn NPs for 20 *ppm* and 10 *ppm* respectively, followed by Zn (18.00) and ZnFe (17.00) for 10 *ppm*. The 20 *ppm* concentration was also found more effective in case of chilli. Similar effects were also observed in case of 50 *ppm* concentration on seed germination. The seed vigour was observed with 20 *ppm* concentration in Zn (67.50) followed by ZnFe (64.16) followed by MnZn (61.66).

**Statistical assessment of seed germination behavior**

Assessing seed germination behavior in tomato, chili and brinjal through SG (%age), MGF and SVI is vital for ensuring seed quality and plant establishment. High SG (%age) indicates viable seeds, while MGF reflects germination speed, crucial for uniform growth. SVI offers a comprehensive measure of seed vigor. Statistical analysis of these parameters provides insights into seed performance, helping breeders and farmers make informed decisions by identifying significant differences among seed lots and varieties.

**Evaluation of seed germination (%age) through regression**

Regression analysis of seed germination data using Minitab revealed key insights. Time (Hrs) positively influenced germination, increasing it by 0.60% per hour, while higher substance concentrations (*ppm*) decreased it by 0.36% per *ppm*. Plant seed type also played a crucial role; *Solanum lycopersicum* and *Solanum melongena* boosted germination by 12.40% and 11.39%, respectively (Table 1). Nanoparticles significantly enhanced germination, with $ZnOFe_2O_3$ showing the highest impact at 20.09%. The model fit was strong, with an *r*-squared value of 79.89%,

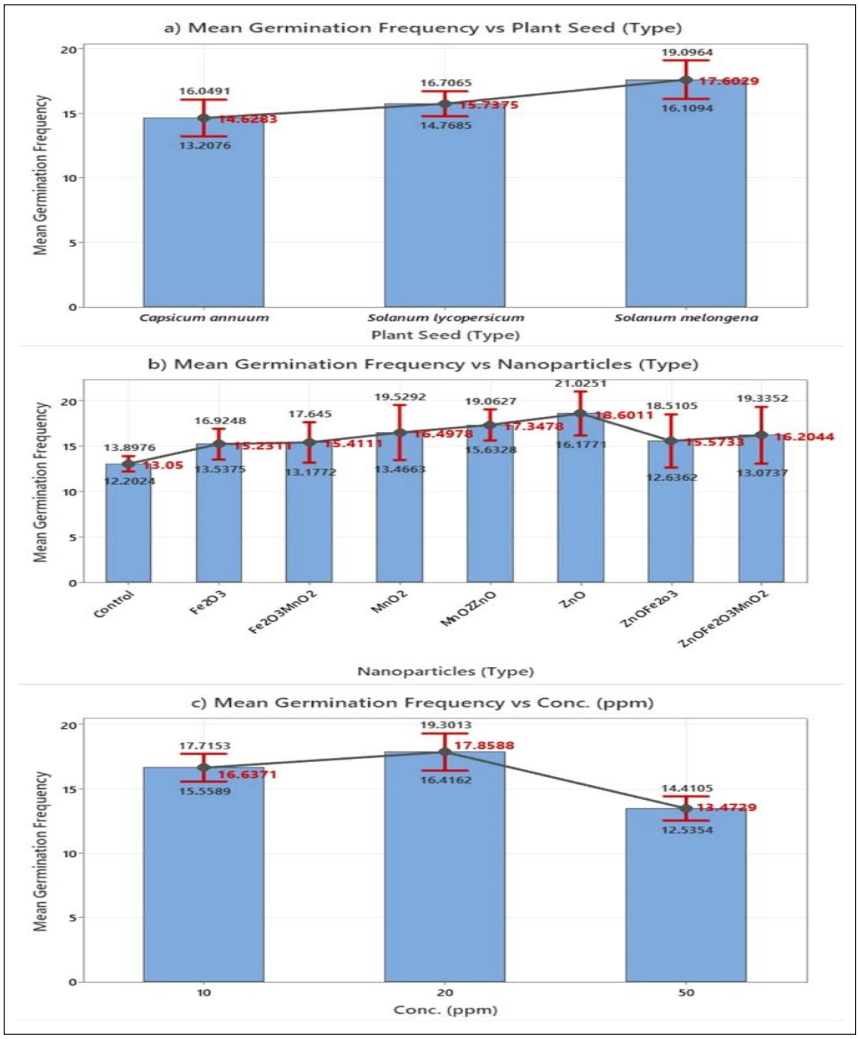



**Fig 5:** Error-bar plots for MGF.

indicating the model explained most variability in seed germination. Statistical analysis confirmed the significance of these factors, providing valuable insights for optimizing seed germination and improving crop yields.

Error bar plots were used to analyze the impact of plant seed (type), time (Hrs), nanoparticle (type) and concentration (*ppm*) on seed germination (percentage). The plots revealed that *Solanum lycopersicum* (66.08%) and *Solanum melongena* (66.37%) had significantly higher germination rates compared to *Capsicum annuum* (54.73%), highlighting the importance of plant seed type (Fig 4). Time also positively influenced germination, with rates increasing from 15.42% at 24 hours to 89.21% at 144 hours. Nanoparticle treatments enhanced germination, with $ZnOFe_2O_3$ showing the highest rate at 71.68%, compared to the control at 50.10%. However, higher concentrations (50 *ppm*) reduced germination to 52.38%, indicating that while moderate concentrations (10-20 *ppm*) were beneficial, excessive amounts could inhibit germination. With *p*-values below 0.05, it was confirmed that plant seed type, time, nanoparticle type and concentration significantly affected seed germination. These findings underscore the importance of optimizing these factors to improve crop yields.

**Assessment of MGF through One-way ANOVA**

One-way ANOVA on mean germination frequency (MGF) revealed significant effects of plant seed (type), nanoparticle (type) and concentration (*ppm*) on germination. For plant seed type, the ANOVA showed significant differences ($p$ = 0.006, $f$ = 5.59), with *Solanum melongena* having the highest mean MGF (17.603), followed by *Solanum lycopersicum* (15.738) and *Capsicum annuum* (14.628). Regarding nanoparticle type, significant differences were found ($p$ = 0.023, $f$ = 2.52), with ZnO yielding the highest mean MGF (18.60) and the control group the lowest (13.050). The analysis of concentration revealed the most substantial differences ($p$ = 0.000, $f$ = 15.95), with 20 *ppm* showing the highest MGF (17.859), while 50 *ppm* had the lowest (13.473). These results highlighted that *Solanum melongena* seeds, ZnO nanoparticles and a concentration of 20 *ppm* were optimal for enhancing seed germination. The findings emphasize the importance of selecting the

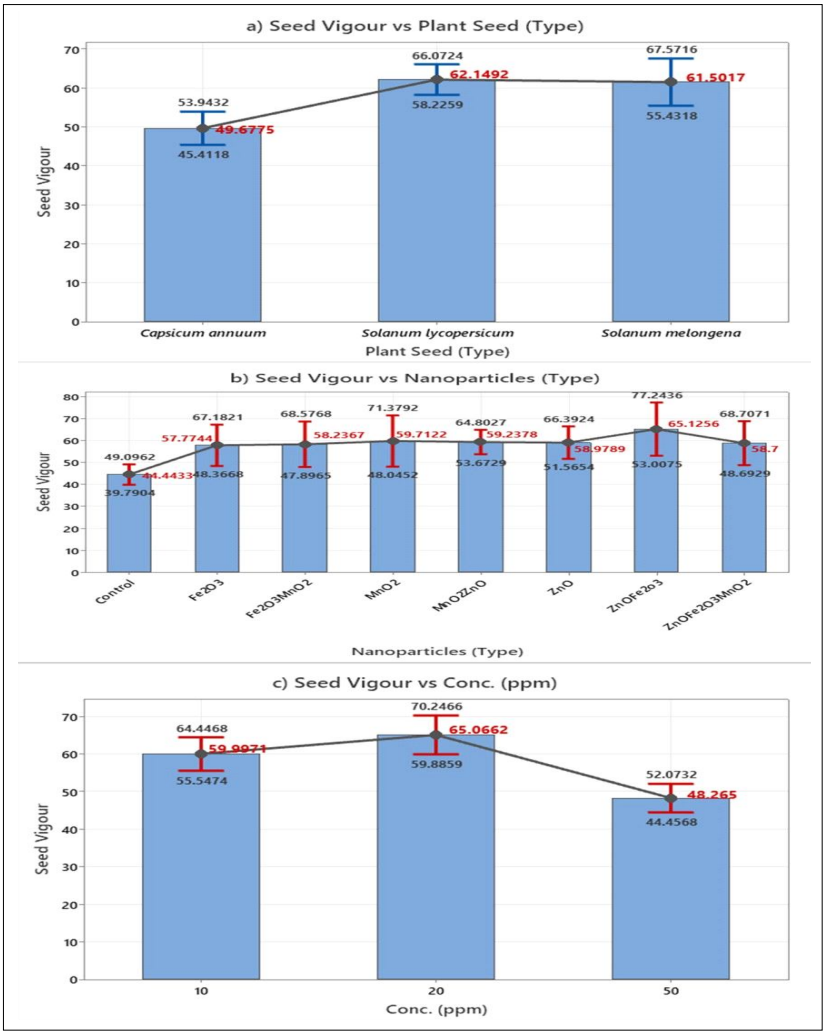



**Fig 6:** Error-bar plots for SVI.

right seed type, nanoparticle treatment and concentration for optimal germination outcomes.

The error-bar plots revealed key insights into MGF with respect to plant seed (type), nanoparticle (type) and concentration (Fig 5). *Solanum melongena* seeds had the highest MGF (~ 19.1) and showed consistent germination performance, outperforming *Solanum lycopersicum* and *Capsicum annuum*. Among nanoparticles, ZnO had the highest MGF (21.0), significantly enhancing seed germination compared to the control group, which had the lowest MGF (13.9). Concentration analysis showed that 20 *ppm* yielded the highest MGF (19.3), while 50 *ppm*, though more variable, resulted in the lowest MGF (14.4). These findings highlighted that *Solanum melongena* seeds, ZnO nanoparticles and a 20 *ppm* concentration were optimal for improving germination, providing valuable guidance for optimizing seed treatment protocols.

**Estimation of SVI through analysis of means**

Seed Vigour Index (SVI) analysis revealed significant differences among plant seed (types) with *Solanum lycopersicum* having the highest mean SVI (62.15), closely followed by *Solanum melongena* (61.50), while *Capsicum annuum* had the lowest (49.68). The analysis of nanoparticles suggested that ZnO$Fe_2O_3$ had the highest mean SVI (65.13), although the differences were not statistically significant (Fig 6). Concentration levels significantly influenced SVI, with 20 *ppm* yielding the highest mean SVI (65.07), followed by 10 *ppm* (60.00). The highest concentration (50 *ppm*) resulted in the lowest SVI (48.27). The findings highlighted that *Solanum* species, ZnO$Fe_2O_3$ nanoparticles and moderate concentrations (20 *ppm*) were optimal for enhancing seed vigour, providing crucial insights for improving seed treatments.

Nano-fertilizers have shown positive effects on seed germination and seedling health, with notable improvements over control groups (Prasad *et al.,* 2012; Madzokere *et al.,* 2021). Research indicates that soaking brinjal, tomato and chili seeds in various nano-fertilizer concentrations significantly boosts growth in a dose-dependent manner. Seeds treated with ZnO, $Fe_2O_3$ and $MnO_2$ NPs generally germinated between the fifth and sixth day, with more intense germination towards the end. ZnO-NPs had varying effects across crop species, with 20 *ppm* concentrations improving seed germination more effectively than 50 *ppm*. García-López *et al.* (2018) observed that while different ZnO NP concentrations did not significantly affect chili seed germination, they notably improved seedling vigor, attributed to zinc nanoparticles' role in auxin synthesis. Green synthesized $Fe_2O_3$ NPs increased the vigor index of tomatoes (Karunakaran *et al.,* 2017; Abusalem *et al.,* 2019).

High NP concentrations may harm seedlings, but low concentrations of ZnO-NPs generally enhance germination and growth, 50 *ppm* ZnO-NPs improved germination. ZnO-NPs also increase root phytohormones, such as IAA, which promote growth (Pandey *et al.,* 2010). Concentrations above 800 *ppm* ZnO-NPs were detrimental to growth and germination (Liu *et al.,* 2015). Topical NP-based nutrients offer a faster, more efficient means of nutrient delivery (Kanwal *et al.,* 2022), with green NPs gaining popularity for their biocontrol efficacy (Hoang *et al.,* 2022; Kumar *et al.,* 2024) and yield (Sharma *et al.,* 2024). Optimizing these parameters enhances agricultural practices and yields, leading to stronger crops and reduced plant competition.

## CONCLUSION

The current study provides an effective and repeatable protocol for the environmentally friendly green synthesis of ZnO, $Fe_2O_3$ and $MnO_2$ NPs and emphasizes its use in enhancing the parameters of brinjal, tomato and chilli seedling growth, vigour, length of the shoot and root. It entered the plant cell quickly and aided in the biomass development of the plant. Therefore, applying NPs to plants that receive the best treatment has a significant impact on crop improvement. It could be a successful technique for increasing seedling development in brinjal, tomato and chilli is to treat seeds with lower concentrations of ZnO, $Fe_2O_3$ and $MnO_2$ NPs (10 and 20 ppm). Additionally, these NPs could be utilized as an easily absorbed type of micronutrient, enhancing agricultural yield and supporting the effective establishment of crops.

**Conflict of interest**

All authors declared that there is no conflict of interest.

## REFERENCES

Arora, V., Singh, B.J., Bithel, N., Malik, N., Upadhyay, S.K. and Singh, R. (2024). Effect of simulated acid rain on plant growth behaviour of *l*Linn. and *Vigna unguiculata* ssp *cylindrica* (L.) *Environmet Development and Sustainability.* **26:** 627-655.

Bala, N., Saha, S., Chakraborty, M., Maiti, M., Das, S., Basu, R. and Nandy, P. (2015). Green synthesis of zinc oxide nanoparticles using Hibiscus subdariffa leaf extract: Effect of temperature on synthesis, anti-bacterial activity and anti-diabetic activity. *RSC. Advances*. **5:** 4993-5003.

Balafrej, H., Bogusz, D., Triqui, Z.E.A., Guedira, A., Bendaou, N., Smouni, A. and Fahr, M. (2020). Zinc hyperaccumulation in plants: A review. *Plants*. **9:** 562.

Abusalem, M., Awwad, A., Ayad, J. and Rayyan, A.A. (2019). Green synthesis of α-$Fe_2O_3$ nanoparticles using pistachio leaf extract influenced seed germination and seedling growth of tomatos. *Jordan Journal of Earth and Environmental Sciences*. **10(3):** 161-166.

Cieschi, M.T., Polyakov, A.Y., Lebedev, V.A., Volkov, D.S., Pankratov, D.A., Veligzhanin, A.A. and Lucena, J.J. (2019). Eco-friendly iron-humic nanofertilizers synthesis for the prevention of iron chlorosis in soybean (*Glycine max*) grown in calcareous soil. *Frontiers in Plant Science*. **10:** 448294.

García-López, J.I., Zavala-García, F., Olivares-Sɑenz, E., Lira-Saldívar, R.H., Díaz Barriga-Castro, E., Ruiz-Torres, N.A. and Niño-Medina, G. (2018). Zinc oxide nanoparticles boosts phenolic compounds and antioxidant activity of *Capsicum annuum* L. during germination. *Agronomy*. **8:** 215.

Gevers, L.E., Enakonda, L.R., Shahid, A., Ould-Chikh, S., Silva, C.I., Paalanen, P.P. and Ruiz-Martínez, J. (2022). Unraveling the structure and role of Mn and Ce for NOx reduction in application-relevant catalysts. *Nature Communications*. **13:** 2960.

Hassanisaadi, M., Barani, M., Rahdar, A., Heidary, M., Thysiadou, A. and Kyzas, G.Z. (2022). Role of agrochemical-based nanomaterials in plants: Biotic and abiotic stress with germination improvement of seeds. *Plant Growth Regulation*. **97:** 375-418.

Hindt, M.N. and Guerinot, M.L. (2012). Getting a sense for signals: Regulation of the plant iron deficiency response. Biochim. Biophys. *Biochimicaet Biophysica Acta (BBA)-Molecular Cell Research*. **1823(9):** 1521-1530.

Hoang, T.K.H., Nguyen, Q.H.V., Nguyen, T.N.H., Tran, T.H. and Le, Q.T.D. (2022). Study on the *in vitro* and *in vivo* antifungal activities of nano-silver against mycoleptodiscus indicus causing leaf blight on lotus in Vietnam. *Indian Journal of Agricultural Research*. **56(6):** 726-733. doi: 10.18805/IJARe.AF-685.

Hoseinpour, V., Souri, M. and Ghaemi, N. (2018). Green synthesis, characterisation and photocatalytic activity of manganese dioxide nanoparticles. *Micro and Nano Letters*. **13:** 1560-1563.

INIC. (2014). Iran Nanotechnology Initiative Council. First nano-organic iron chelated fertilizer invented in Iran http://www.iranreview.org/content/Documents/Iranians_Researchers_Produce_Nano_Organic_Fertilizer.htm.

Kajbafvala, A., Ghorbani, H., Paravar, A., Samberg, J.P., Kajbafvala, E. and Sadrnezhaad, S.K. (2012). Effects of morphology on photocatalytic performance of Zinc oxide nanostructures synthesized by rapid microwave irradiation methods. *Superlattices Microstruct*. **51:** 512-522.

Kanwal, A., Sharma, I., Bala, A., Upadhyay, S.K. and Singh, R. (2022). Agricultural application of synthesized ZnS nanoparticles for the development of tomato crop. *Letters in Applied Nano Bio Science*. **12:** 1-9.

Karunakaran, G., Jagathambal, M., Van Minh, N., Kolesnikov, E., Gusev, A., Zakharova, O.V. and Kuznetsov, D. (2017). Green synthesized iron oxide nanoparticles: A nano-nutrient for the growth and enhancement of flax (*Linum usitatissimum* L.) plant. *Indian Journal of Biochemistry and Biophysics*. **11:** 289-293.

Keshri, S. and Biswas, S. (2022). Synthesis, physical properties and biomedical applications of magnetic nanoparticles: A review. *Progress in Biomaterials*. **11:** 347-72.

Khaleghi, S., Khayatzadeh, J. and Neamati, A. (2022). Biosynthesis of zinc oxide nanoparticles using *Origanum majorana* L. leaf extract, its antioxidant and cytotoxic activities. *Materials and Technology Journal*. **37:** 2522-2531.

Kumar, M., Saini, R.V., Gupta, M. and Singh, R. (2024). Green synthesis of silver nanoparticle (Cha-AgNPs) using Chenopodium album extract and evaluation of their antifungal potential against pathogenic fungi. *Biomass Convers. Biorefin.* https://doi.org/10.1007/s13399-024-05721-z.

Kumar, S., Arora, D., Dhupar, A., Sharma, V., Sharma, J.K., Sharma, S.K. and Gaur, A. (2020). Structural and optical properties of polycrystalline ZnO nanopowder synthesized by direct precipitation technique. *Journal of Nano- and Electronic Physics*. **12:** 04027.

Lin, J., He, F., Su, B., Sun, M., Owens, G. and Chen, Z. (2019). The stabilizing mechanism of cadmium in contaminated soil using green synthesized iron oxide nanoparticles under long-term incubation. *Journal of Hazardous Materials*. **379:** 120832.

Liu, X., Wang, F., Shi, Z., Tong, R. and Shi, X. (2015). Bioavailability of Zn in ZnO nanoparticle-spiked soil and the implications to maize plants. *Journal of Nanoparticle Research*. **17:** 1-11.

Madzokere, T.C., Murombo, L.T. and Chirириwa, H. (2021). Nano-based slow releasing fertilizers for enhanced agricultural productivity. *Materials Today: Proceedings*. **45:** 3709-3715.

Narayanamma, A., Rani, A. and Raju, M.E. (2016). Natural synthesis of silver nanoparticles by banana peel extract and as an antibacterial agent. *IOSR Journal of Polymer and Textile Engineering*. **3:** 17-25.

Ogunyemi, S.O., Zhang, F., Abdallah, Y., Zhang, M., Wang, Y., Sun, G. and Li, B. (2019). Biosynthesis and characterization of magnesium oxide and manganese dioxide nanoparticles using *Matricaria chamomilla* L. extract and its inhibitory effect on Acidovorax oryzae strain RS-2. Artif Cells. *Nanomedicine and Biotechnology*. **47:** 2230-2239.

Pandey, A.C., Sanjay, S. and Yadav, R. (2010). Application of ZnO nanoparticles in influencing the growth rate of Cicer arietinum. *Journal of Experimental Nanoscience*. **5:** 488-497.

Prasad, T.N.V.K.V., Sudhakar, P., Sreenivasulu, Y., Latha, P., Munaswamy, V., Reddy, K.R. and Pradeep, T. (2012). Effect of nanoscale zinc oxide particles on the germination, growth and yield of peanut. *Journal Plant Nutrition*. **35:** 905-927.

Renna, M., Durante, M., Gonnella, M., Buttaro, D., D'Imperio, M., Mita, G. and Serio, F. (2018). Quality and nutritional evaluation of regina tomato, a traditional long-storage landrace of puglia (Southern Italy). *Agriculture*. **8:** 83.

Sharma, G., Rana, A. and Sharma, A. (2024). Impact and assessment of engineered metallic nano-oxide on the growth and development of *Gossypium hirsutum* L. *Indian Journal of Agricultural Research*. **58(1):** 89-94. doi: 10.18805/IJARe.A-5872.

Shatnawi, M., Alsmadi, A.M., Bsoul, I., Salameh, B., Mathai, M., Alnawashi, G., Alzoubi, G.M., Al-Dweri, F. and Bawa'aneh, M.S. (2016). Influence of Mn doping on the magnetic and optical properties of ZnO nanocrystalline particles. *Results in Physics*. **6:** 1064-71.

Sheoran, P., Grewal, S., Kumari, S. and Goel, S. (2024). Effect of environmentally benign nano-nitrogen, potassium, zinc on growth and yield enhancement in *Triticum aestivum*. *Indian Journal of Agricultural Research*. **58(3):** 480-483. doi: 10.18805/IJARe.A-5698.

Siddiqui, M.H. and Al-Whaibi, M.H. (2014). Role of nano-$SiO_2$ in germination of tomato (*Lycopersicum esculentum seeds Mill*.). *Saudi Journal of Biological Sciences*. **21:** 13-17.

Thi Tran, Q.M., Thi Nguyen, H.A., Doan, V.D., Tran, Q.H. and Nguyen V.C. (2021). Biosynthesis of zinc oxide nanoparticles using aqueous piper beetle leaf extract and its application in surgical sutures. *Journal of Nanomaterials*. 1-15.

Üstün, E., Önbaş, S.C., Çelik, S.K., Ayvaz, M.Ç. and Şahin, N. (2022). Green synthesis of iron oxide nanoparticles by using *Ficus carica* leaf extract and its antioxidant activity. *Biointerface Research in Appllied Chemistry*. **12:** 2108-2116.

Wang, X., Ding, Y., Summers, C.J. and Wang, Z.L. (2004). Large-scale synthesis of six-nanometer-wide ZnO nanobelts. *Journal of Physical Chemistry B*. **108(26):** 8773-8777.